Anca DIDU, Andra CONSTANTIN, Violeta CONTOLORU, Cristina ROTEA, Gabriel MARINESCU

COMPUTER-AIDED GRAPHICS IN THE DESIGN OF MOBILE MECHANICAL SYSTEMS

Abstract: *There are presented analytical and virtual prototyping methods for the kinematic study of the mechanism from an industrial robot with 5 degrees of freedom. The authors are interested in the analytical and graphical identification of the work space, including the kinematic parameters, which are necessary in the geometric modeling of the kinematic couplings. The virtual prototyping for a worm gear that forms a rotation coupler from the robot structure has been made. Adams and ALGOR programs were used.*

Key words: *finite elements, virtual prototyping, mathematical modelling, powder metallurgy.*

1. INTRODUCTION

A mechanism from a robot with 5 degrees of freedom is analyzed, which has two components, namely the trajectory generating mechanism and the orientation mechanism. Two structural variants from the point of view of the trajectory generator are studied. The analytical method for identifying the workspace is based on a relatively simple, flexible and computational matrix formalism [1,2,3].

For the virtual prototyping of the worm gear, the finite element method was used [4,6]. It is to be noted that the worm gear was made by powder metallurgy of an antifriction alloy.

Improving the technologies of elaboration of Powder Metallurgy (MP) of high mechanical strength parts from sintered steels is also a major concern of researchers at present.

The materials obtained through powder metallurgy offer many advantages and are used in construction for various means of transport (cars, trains, planes). These types of materials, largely represented by iron, copper and aluminum, are obtained by pressing and sintering metallic powders with the addition of binders and other necessary materials.

2. THE KINEMATIC ANALYSIS OF THE ROBOTIC ARM

2.1 The analytical method

The M point position in relation to the global reference system T_0 is:

$$\vec{r}_{T_0}^{\,M} = \vec{r}_1 + \vec{\delta}_1 + \vec{\delta}_2 + \vec{r}_3 + \vec{\delta}_4 + \vec{r}_5 + \vec{S}_5$$

$$\vec{\delta}_2 = \{\delta_2\}^T W_1;$$

$$\vec{r}_3 = \{r_3\}^T \vec{W}_2;$$

$$\vec{r}_5 = \{r_5\}^T \{\vec{W}_4\};$$

$$\vec{\delta}_5 = \{S_5\}^T \{\vec{W}_5\} \qquad (1)$$

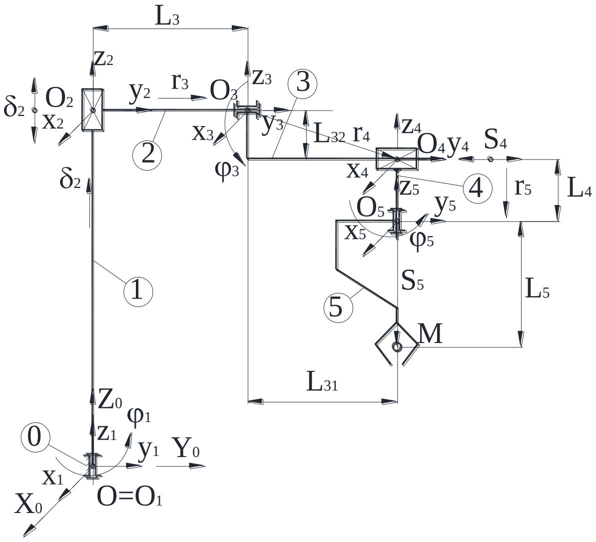

Fig. 1 The kinematic scheme of the robot.

The transformation matrices of the coordinates are introduced in the transition from one reference system to another based on the fundamental relationship:

$$\vec{W}_{1-i} = [A_{01-1}]\vec{W}_0 \qquad (2)$$

$$\vec{W}_1 = [A_{01}]\vec{W}_0 \qquad (3)$$

$$\vec{W}_2 = [A_{12}]\vec{W}_1 = [A_{12}][A_{01}]\vec{W}_0 \qquad (4)$$

$$\vec{W}_3 = [A_{23}]\vec{W}_2 = [A_{23}][A_{12}][A_{01}]\vec{W}_0 \qquad (5)$$

$$\vec{W}_4 = [A_{34}]\vec{W}_3 = [A_{34}][A_{23}][A_{12}][A_{01}]\vec{W}_0 \qquad (6)$$

$$\vec{W}_5 = [A_{45}]\vec{W}_4 = [A_{45}][A_{04}]\vec{W}_0 \qquad (7)$$

Position of the point O_2 in relation to the reference system T_0 is:

$$\vec{r}_{T_0}^{\,O_2} = \{\delta_2\}^T \vec{W}_1 = \{\delta_2\}^T [A_{01}]\vec{W}_0 \qquad (8)$$

Position of the point O_3 in relation to the reference system T_0 is:

$$\vec{r}_{T_0}^{O_3} = \vec{\delta}_2 + \vec{r}_3 = \{\delta_2\}^T \vec{W}_1 + \{r_3\}^T \vec{W}_2 = \\ = \{\delta_2\}^T [A_{01}] \vec{W}_0 + \{r_3\}^T [A_{02}] \vec{W}_0 \qquad (9)$$

Position of the point O_4 in relation to the reference system T_0 is:

$$\vec{r}_{T_0}^{O_4} = \vec{\delta}_2 + \vec{r}_3 + \vec{\delta}_4 = \{\delta_2\}^T [A_{01}] \vec{W}_0 + \\ + \{r_3\}^T [A_{02}] \vec{W}_0 + \{\delta_4\}^T [A_{03}] \vec{W}_0 \qquad (10)$$

Position of the point O_5 in relation to the reference system T_0 is:

$$\vec{r}_{T_0}^{O_5} = \vec{\delta}_2 + \vec{r}_3 + \vec{\delta}_4 + \vec{r}_5 = \\ \{\delta_2\}^T [A_{01}] \vec{W}_0 + \{r_3\}^T [A_{02}] \vec{W}_0 + \\ + \{\delta_4\}^T [A_{03}] \vec{W}_0 + \{r_5\}^T [A_{04}] \vec{W}_0 \qquad (11)$$

The coordinate transformation matrices:

$$[A_{01}] = \begin{bmatrix} \cos\varphi_1 & -\sin\varphi_1 & 0 \\ \sin\varphi_1 & \cos\varphi_1 & 0 \\ 0 & 0 & 1 \end{bmatrix}; \qquad (12)$$

$$[A_{12}] = \begin{bmatrix} 1 & 0 & 0 \\ 0 & 1 & 0 \\ 0 & 0 & 1 \end{bmatrix} ; \qquad (13)$$

$$[A_{23}] = \begin{bmatrix} \cos\varphi_3 & 0 & -\sin\varphi_3 \\ 0 & 1 & 0 \\ \sin\varphi_3 & 0 & \cos\varphi_3 \end{bmatrix} \qquad (14)$$

$$[A_{34}] = \begin{bmatrix} 1 & 0 & 0 \\ 0 & 1 & 0 \\ 0 & 0 & 1 \end{bmatrix}; \qquad (15)$$

$$[A_{45}] = \begin{bmatrix} \cos\varphi_5 & -\sin\varphi_5 & 0 \\ \sin\varphi_5 & \cos\varphi_5 & 0 \\ 0 & 0 & 1 \end{bmatrix}; \qquad (16)$$

$$\{\vec{\delta}_2\} = [0,0,S_2]^T \quad ; \{\vec{r}_3\} = [0,L_2,0]^T \\ \{\vec{\delta}_4\} = [0,L_{31},-L_{32}]^T \ ; \{\vec{r}_5\} = [0,0,-L_4]^T \\ \{S_5\} = [0,0,-L_5]^T \qquad (17)$$

2.2 Mathematical models processing

A program was created under the Maple programming environment, with the following input data:

- geometric data:

$L_2 = 400; L_{32} = 200; L_4 = 400; L_5 = 300;$

Generalized coordinates: $(S_2, S_3, \varphi_1, \varphi_3, \varphi_5)$

Time variation laws of generalized coordinates:

$$S_2 = 30 \cdot t; S_3 = 10 \cdot t; \varphi_1 = 4.24 \cdot t; \\ \varphi_3 = 0.4712 \cdot t; \varphi_5 = 0.314 \cdot t;$$

The positions, speeds and accelerations for each kinematic element or characterisic point of the robot are determined:

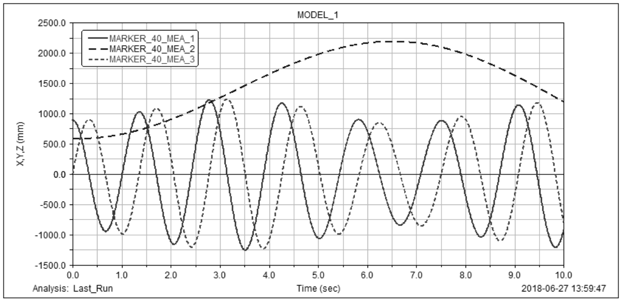

Fig. 2 The variation laws of the components along the axes x, y, z for the position vector of the characteristic point.

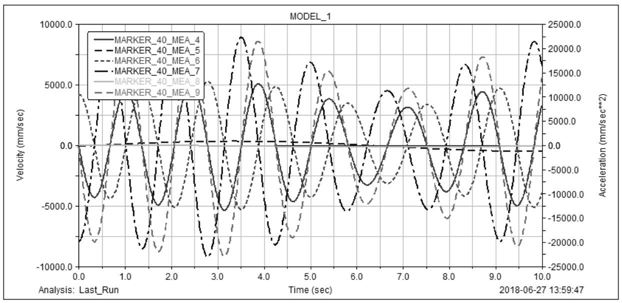

Fig. 3 The variation laws of the components along the axes x, y, z for the velocity vector of the characteristic point.

2.3 Numerical simulation with Adams program

With numerical data and variation laws of generalized coordinates defined in the mathematical model, two kinetic variants of the robot are built with the Adams program. It identifies the working space in the two structural variants, the time variation laws for the kinematic parameters and the connecting forces in the joints. These forces are useful in dimensioning the mechanical transmissions that constructively model the couplers in the mechanical system.

Each scheme consists of 5 mobile kinematic elements connected by 5 motor kinematic couplers.

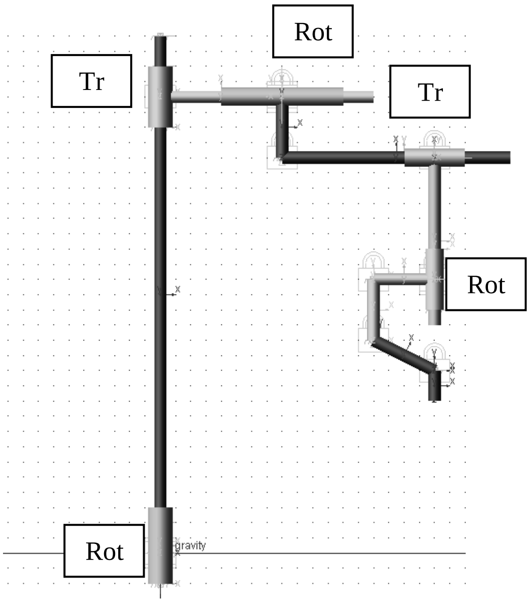

Fig. 4 Kinematic scheme with the RTR trajectory generator mechanism.

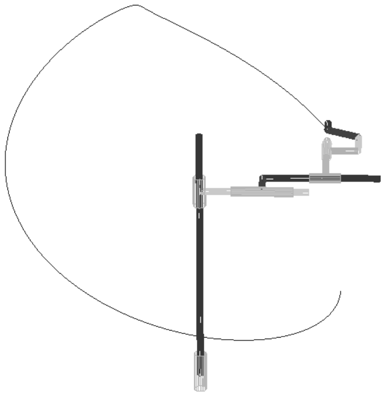

Fig. 5 Numerical 3D simulation with the RTR generator.

Fig. 6 The kinematic scheme in successive positions, with the RTR generator mechanism**.**

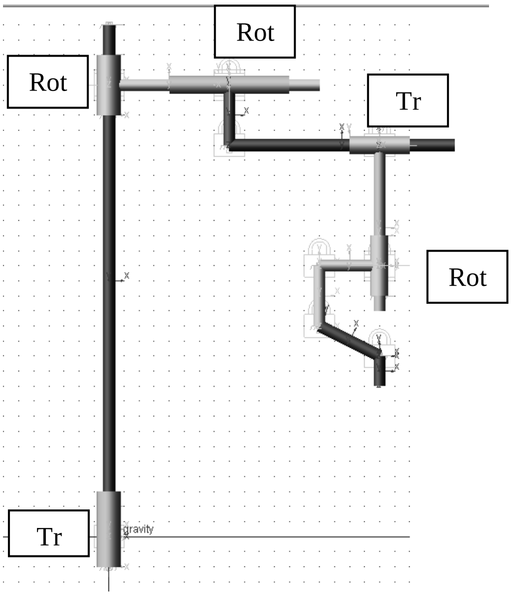

Fig. 7 The kinematic scheme with the TRR trajectory mechanism.

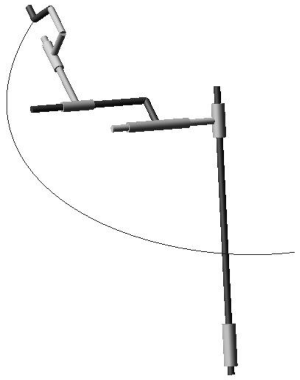

Fig. 8 3D numerical simulation with the TRR generator mechanism**.**

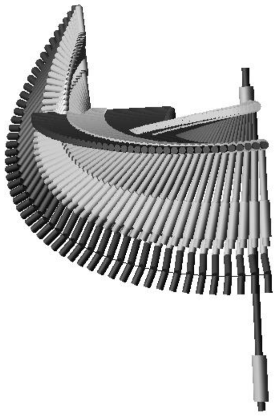

Fig. 9 The kinematic scheme in successive positions**.**

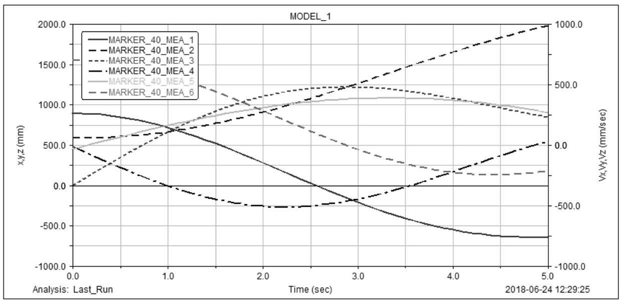

Fig. 10 The variation laws of the components along the axes x, y, z for the position and speed of the characteristic point M.

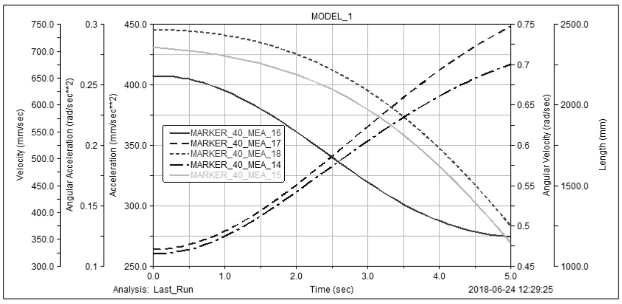

Fig. 11 The variation laws of x, y and z axes for linear and angular speeds of the characteristic point M.

The processed numeric data are valid for the scheme in figure 1.

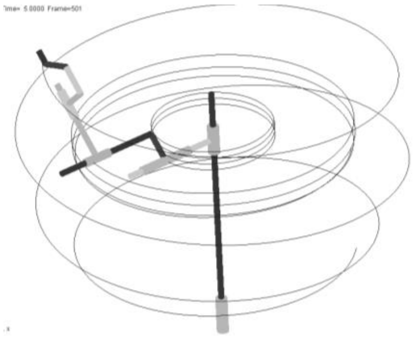

Fig. 12 Workspace for the RTRTR system.

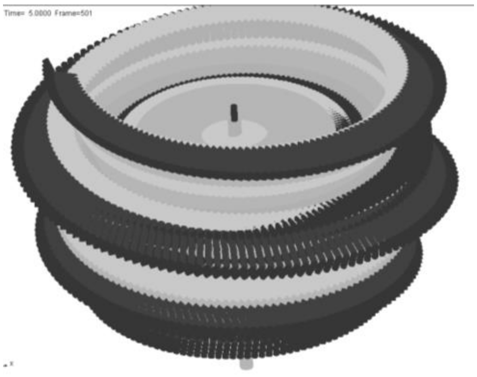

Fig. 13 The RTRTR mechanism in successive positions**.**

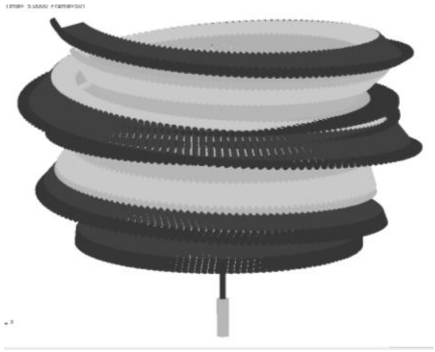

Fig. 14 RTRTR mechanism in successive positions (front view).

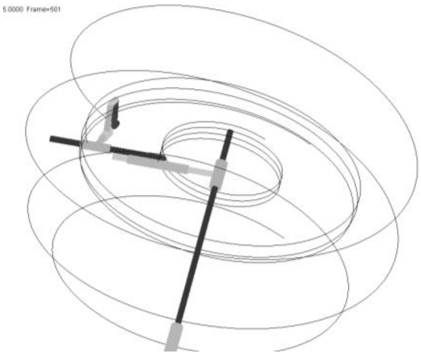

Fig. 15 Workspace for the RTRTR system (rotary view).

Fig. 16 Workspace for the TRRTR system.

Fig. 17 The TRRTR mechanism in successive positions.

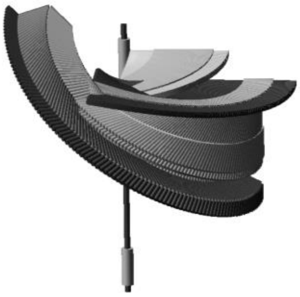

Fig. 18 The TRRTR mechanism in successive positions.

Fig. 19 The TRRTR mechanism in successive positions.

Fig. 20 The sequence in the workspace for the TRRTR mechanism in successive positions.

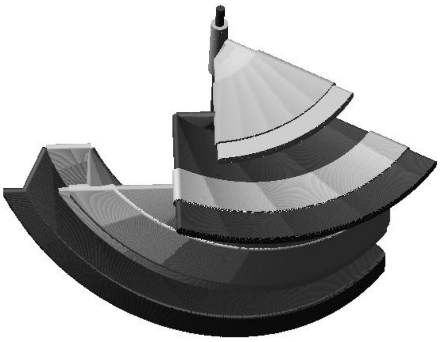

Fig. 21 The sequence in the workspace for the TRRTR mechanism in successive positions.

2.4 Finite element modeling of worm gear for actuation of rotation coupler b [5,7,8].

Design data:

- Rated power to be transmitted P=0,704 Kw ;
- Worm speed n = 100 rpm;
- Gearing ratio I = 30;
- Materials: cast iron,the worm wheel and an alloy of metallic powders with antifriction properties for the worm gear.
- From the contact fatigue strength condition, the distance between the axes $a_w = 62.5$ mm was determined and the bending strength condition determined the axial module $m_x = 2.5$ mm.
- Geometrical elements:

$Z_w = 1$ number of beginnings for the worm;

$Z_2 = 30$ the number of worm wheel teeth;

$q = 10$ the diametral coefficient;

$d_1 = 25$ the pitch diameter of the worm;

$d_2 = 75$ the pitch diameter of the worm wheel

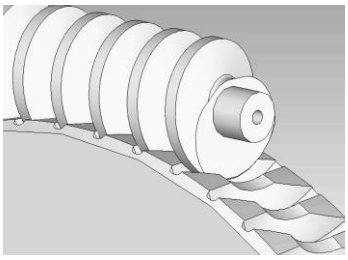

Fig. 22 Worm gearing in 3D (detail)

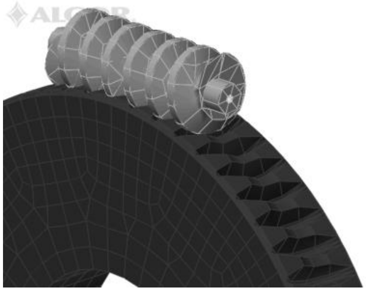

Fig. 23 Geometric model and rotation couplers for the worm and the worm wheel (detail)

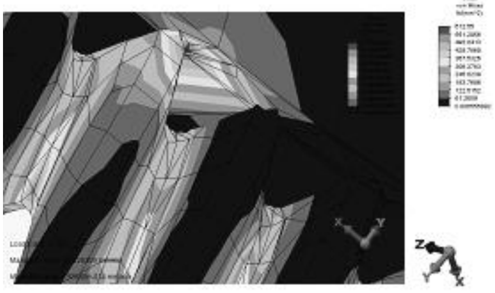

Fig. 24 Distributions of Von Mises equivalent deformations for the gear.

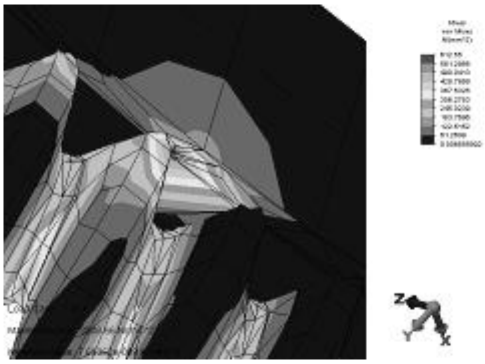

Fig. 25 Distribution of Von Mises equivalent tensions for the wheel.

3. CONCLUSIONS

For the inverse dynamic analysis of the mechanism from an industrial robot with 5 degrees of freedom, the following steps were taken:

- Elaboration of the kinematic scheme for the trajectory generator mechanism and the orientation mechanism;
- Establishment of time variation laws of generalized coordinates;
- Mathematical modeling of the robot working space through direct kinematic analysis;
- Developing the kinematic model based on the theory of multi-body systems with the Adams program;
- Identification of time variation laws for kinematic parameters (positions, speeds, accelerations);
- Numerical processing and simulation of the working space;

The finite element analysis of the worm gear was performed as follows:

- Worm gear design and 3D geometric design;
- Modeling of worm and worm wheel rotation coupler with finite bar type elements;
- Definition of the material properties, the loads and the meshing with finite elements of the geometric model;
- Determining the distribution of displacements, deformations and stresses in the gear elements.

The following results were obtained:

1. The trajectory of the characteristic point M, attached to the mechanical hand is a spatial curve for both versions of the robot's kinematic schemes (Figures 5,12,15 and Figures 8,16).
2. Mathematical models and numerical simulation materialized by presentations in successive positions, which highlight the continuity of movement for the two kinematic chains, respectively the generator of trajectories and the orientation one (fig. 6, fig. 13, fig. 14 and fig. 17, fig. 18- fig. 21).
3. In the finite element analysis of the worm gearing is important the modeling of the rotation couplers for the worm and the worm gear, through finite elements type bars, that allow the loading with the torsion moment of the worm.
4. Relatively high values of stresses are mainly recorded in the area of the virtual model of the two joints without practical effects.
5. The stresses and deformations in the contact area have values that enclose in the permissible limits (σ_{max}= 700 MPa).
6. The analyzed part is obtained through Powder Metallurgy and has properties similar to those obtained by classical technologies.

REFERENCES

[1] Bauchau O.A., *Flexible Multibody Dynamics*, Springer,2011.

[2] Charles E.W., Sadler,P., *Kinematics and dynamics of machinery*, Harper Collins College Publishers, 1993.

[3] Dumitru, N., Nanu, Gh.,Vintila, D., *Mechanisms and mechanical transmissions*, Ed. Didactics and Pedagogy, Craiova, 2008.

[4] Dumitru, N., *Mobile mechanical systems*. Virtual prototyping and experimental analysis, Ed. Universitaria,2018.

[5] Faydor Litvin, *Gears geometry*, Ed. Dacia ,2009.

[6] Saed Moaveni, *Finite Element Analysis*, Parson Education, 2003.

[7] Robert, L., Norton, *Design of Mashinery*, McGraw Hill, 2008.

[8] Robert C. Juvinal, *Fundamentals of Mashine Component Design*, John Willey &Sons, 1999.

Authors:

Anca DIDU, University Assistant, University of Craiova, Faculty of Mechanics, E-mail: ankadidu11@gmail.com.

Andra CONSTANTIN, PhD student, University of Craiova, Faculty of Mechanics, E-mail: constantinralucaandra@yahoo.com.

Violeta CONTOLORU, University Lecturer, University of Craiova, Faculty of Mechanics, E-mail: dumitru.violeta@yahoo.com.

Cristina ROTEA, University Lecturer, University of Craiova, Faculty of Mechanics, E-mail: ccploscaru@yahoo.ro.

Gabriel MARINESCU, University Assistant, University of Craiova, Faculty of Mechanics, E-mail: gabrielcatalinmarinescu@gmail.com.